NIRS-SPM: Statistical Parametric Mapping for Near Infrared Spectroscopy

Sungho Tak[a], Kwang Eun Jang[a], Jinwook Jung[a], Jaeduck Jang [a], Yong Jeong[a], Jong Chul Ye[a]

[a]Bio-Imaging and Signal Processing Lab. Dept. of Bio and Brain Engineering
Korea Advanced Institute of Science and Technology (KAIST)
373-1 Guseong-dong Yuseong-gu, Daejon, Korea

ABSTRACT

Even though there exists a powerful statistical parametric mapping (SPM) tool for fMRI, similar public domain tools are not available for near infrared spectroscopy (NIRS). In this paper, we describe a new public domain statistical toolbox called NIRS-SPM for quantitative analysis of NIRS signals. Specifically, NIRS-SPM statistically analyzes the NIRS data using GLM and makes inference as the excursion probability which comes from the random field that are interpolated from the sparse measurement. In order to obtain correct inference, NIRS-SPM offers the pre-coloring and pre-whitening method for temporal correlation estimation. For simultaneous recording NIRS signal with fMRI, the spatial mapping between fMRI image and real coordinate in 3-D digitizer is estimated using Horn's algorithm. These powerful tools allows us the super-resolution localization of the brain activation which is not possible using the conventional NIRS analysis tools.

Keywords: near infared spectroscopy, general linear model, statistical parametric mapping, excursion probability, inhomogeneous Gaussian random filed, tube formula

1. INTRODUCTION

Near infrared spectroscopy (NIRS) is a non-invasive method to measure the brain activity as the changes of hemoglobin oxygenation through the intact skull.[1] Near infrared light between 650 and 950 nm is much less absorbed by biological tissue, and the absorption spectra of oxy-hemoglobin (HbO_2) and deoxy-hemoglobin (HbR) are different in this region.[2] Using this property, it is possible to determine the concentration change of oxy- and deoxy-hemoglobin from diffusely scattered light.

Recently, many researchers have been developing statistical analysis toolbox for NIRS based on generalized linear model (GLM).[3–5] GLM is a statistical linear model that explains data as a linear combination of an explanatory variable plus an error term. Because GLM measures the temporal variational pattern of signals rather than their absolute magnitude, GLM is robust to many cases even with a severe optical signal attenuation due to scattering or poor contact. Since this statistical parameter mapping (SPM) using GLM has become the standard method for analyzing the fMRI data,[6] an integration of NIRS and fMRI within the same SPM framework has an advantage with modeling both types of data in the same mathematical framework to make the classical inference.

Recently, Koh et al.[5] have developed an extensive statistical NIRS analysis tools called functional optical signal analysis (fOSA), which applies the SPM method to NIRS data. They showed that most of the SPM framework can be successfully applied to NIRS data with slight modification. However, several fundamental issues still remain unsolved. For example, even though Gaussian random field theory has been used and justified in fOSA as a tool for inference, the basic assumption for Gaussian random field model breaks down in NIRS. Recall that SPM for fMRI analysis assume that the residuals after the GLM fitting are *dense* samples on lattice representations from an underlying continuous Gaussian random field[7] due to the Gaussian kernel smoothing. However, because the distance between each channel of NIRS is far and the number of measurements are sparse, it is not reasonable to use Gaussian random field theory in making inference of NIRS data. Furthermore, the

Further author information: (Send correspondence to Jong Chul Ye)
Jong Chul Ye: E-mail: jong.ye@kaist.ac.kr, Telephone: +82-42-869-4320

Multimodal Biomedical Imaging III, edited by Fred S. Azar, Xavier Intes,
Proc. of SPIE Vol. 6850, 68500T, (2008)
1605-7422/08/$18 · doi: 10.1117/12.762291

resolution of fOSA is limited by the distance between the optode, which makes it difficult to co-registrate with fMRI activation map.

The main contribution of this article is a new theory for statistical inference and the corresponding public domain software called NIRS-SPM. While the SPM for fMRI calculates the excursion probability of the *homogenous* Gaussian random field by *smoothing* samples on *dense* lattice, NIRS requires excursion probability of *inhomogenous* Gaussian random field obtained by *interpolating* samples on *sparsely* and *irregularly* distributed optode locations. Even though excursion probability for inhomogeneous random field is extremely difficult to calculate in general, the excursion probability for strikingly similar inhomogeneous random field model has been studied for the so-called global confidence region analysis of 3-D parametric shape estimation problem[8] using Sun's tube formula.[9] For example, the p- value for the one side t- test for oxy- or deoxy- hemoglobin concentration can be converted into the excursion probability of Gaussian random field on a two dimensional *representation manifold* that is dependent on the structure of covariance matrix and the interpolating kernels. Furthermore, we can extend the result to calculate p-value of the simultaneous activation of oxy- and deoxy- hemoglobin signals by calculating an excursion probability of Gaussian random field on a three dimensional representation manifold. Thanks to these powerful tools for excursion probability, NIRS-SPM enables super-resolution localization of the brain activation, which was not possible using any other conventional methods such as fOSA.

This paper also describes several other techniques to optimize our NIRS-SPM. First, in estimating the temporal correlations, we compare the pre-coloring and pre-whitening methods introduced in fMRI model.[10] Even though the pre-whitening method is the most efficient approach to parameter estimation and currently implemented in SPM, the difference between the assumed and the actual correlations can produce some bias that make profound effects in inference. Hence, the appropriate method for estimating the temporal correlations in NIRS data has been proposed. Second, in order to localize the NIRS signal to the cerebral cortex of anatomical T1 image which is obtained from MRI, Horn's algorithm[11] is implemented in NIRS-SPM. Finding the relationship between the real 3-D space and the MR image domain using pairs of coordinates in both systems is a well known problem called as absolute orientation. A closed-form, least-square solution for this problem is implemented as described in Horn (1987).[11]

2. STATISTICAL PARAMETRIC MAPPING FOR NEAR INFRARED SPECTROSCOPY

2.1 Measurement Model for NIRS

The modified Beer-Lambert law (MBLL) which describes an optical attenuation in a highly scattering medium like biological tissue allows the transformation from raw optical density (OD) data to changes of chromophore concentrations. According to the MBLL, the change in $OD(\lambda, r, t)$ at the wavelength λ from the cerebral cortex position r at time t due to the N_c number of chromophore concentration changes $\{\Delta c^{(i)}(r,t)\}_{i=1}^{N_c}$ is described as

$$\triangle OD(\lambda, r, t) = -ln\left(\frac{I_F}{I_o}\right) = \sum_{i=1}^{N_c} a_i(\lambda) \triangle c^{(i)}(r,t) d(r) l(r), \tag{1}$$

where I_F denote the final measured optical intensity, I_o denotes the initial measured optical intensity, $a_i(\lambda)$ is the extinction coefficient of the i-th chromophore at the wavelength λ, $d(r)$ is the differential pathlength factor (DPF) at the position r, respectively. Assuming that oxy- and deoxy- hemoglobin are the major two choromophores, the noisy measured optical density changes are then described as follow:

$$\begin{bmatrix} \Delta OD(r,t;\lambda_1) \\ \Delta OD(r,t;\lambda_2) \end{bmatrix} = d(r)l(r) \begin{bmatrix} a_1(\lambda_1) & a_2(\lambda_1) \\ a_1(\lambda_2) & a_2(\lambda_2) \end{bmatrix} \begin{bmatrix} \Delta c_{HbO_2}(r,t) \\ \Delta c_{HbR}(r,t) \end{bmatrix} + \begin{bmatrix} w(r,t;\lambda_1) \\ w(r,t;\lambda_2) \end{bmatrix} \tag{2}$$

where $\Delta c_{HbO_2}(r,t), \Delta c_{HbR}(r,t)$ denote the time-series of the chromophore changes for the oxy- and deoxy-hemoglobin; and $w(r,t;\lambda_1), w(r,t;\lambda_2)$ are the additive noise at the wavelength λ_1 and λ_2, respectively. Then, by multiplying the inverse matrix of the extinction coefficients with Eqn. (2), we have the noisy measurement of oxy- and deoxy- hemoglobin concentration changes:

$$\begin{bmatrix} y_{HbO}(r,t) \\ y_{HbR}(r,t) \end{bmatrix} = d(r)l(r) \begin{bmatrix} \Delta c_{HbO}(r,t) \\ \Delta c_{HbR}(r,t) \end{bmatrix} + \begin{bmatrix} \epsilon_{HbO}(r,t) \\ \epsilon_{HbR}(r,t) \end{bmatrix} \tag{3}$$

where $\epsilon_{HbO_2}(r,t)$ and $\epsilon_{HbR}(r,t)$ are additive zero mean Gaussian noise for oxy- and deoxy- channel. In practice, it is impossible to measure the exact value of $d(r)$ and $l(r)$. This is because that the NIRS data acquisition is considerably affected by variety of measurement conditions such as the color of hair and the scalp depth, which make the position- and subject- dependent scattering effect. Non-uniform contact between optodes and a scalp might be another source of the variation of sensitivities of detectors. There are other experimental issues such as the subject's movement during the experiment. For these reasons, analyzing NIRS data with the absolute value of chromophore concentration is problematic.

2.2 General Linear Model for NIRS

In this section, we mainly focus on the GLM for the oxy-hemoglobin concentration. Exactly same approach can be applied for deoxy-hemoglobin concentration.

Let $\mathbf{y}_{HbO_2}^{(i)} \in \mathbb{R}^N$ and $\boldsymbol{\epsilon}_{HbO_2}^{(i)} \in \mathbb{R}^N$ denote the time series of the oxy- hemoglobin signal and noise at the i-th channel at the location r_i. given by: Then, corresponding GLM model is given by

$$\mathbf{y}_{HbO_2}^{(i)} = \mathbf{X}_{HbO_2}\boldsymbol{\beta}_{HbO_2}^{(i)} + \boldsymbol{\epsilon}_{HbO}^{(i)}, \tag{4}$$

where $\mathbf{X}_{HbO_2} \in \mathbb{R}^{N\times M}$ denotes the design matrices for oxy-hemoglobin, and $\boldsymbol{\beta}_{HbO_2}^{(i)} \in \mathbb{R}^{M\times 1}$ is the corresponding response signal strength at the i-th channel, respectively. The interpolated t- statistics is given by

$$T_{HbO_2}(r) = \frac{\sum_{i=1}^{K} b_i(r)\mathbf{c}^T\boldsymbol{\beta}_{HbO_2}^{(i)}}{\sqrt{\sum_{i=1}^{K} b_i^2(r)\sigma_{HbO_2}^{(i)2}\left(\mathbf{c}^T\mathbf{X}_{HbO_2}^{\dagger}\boldsymbol{\Lambda}_{HbO_2}\mathbf{X}_{HbO}^{\dagger T}\mathbf{c}\right)}} \tag{5}$$

where $b_i(r)$ denotes the i-th interpolation kernel and $\sigma_{HbO_2}^{(i)2}$ the signal variance at the i-th channel, and $\mathbf{c}$ denotes the contrast vector.

2.3 Inference using Global Confidence Region Analysis

The p-value of the t- statistics to abandon null hypothesis is given by

$$p \quad = \quad P\left\{\max_{r\in\Psi} T_{HbO_2}(r) \geq z\right\} \tag{6}$$

Ye et al.(2006)[8] derived the two approximation for the probability in Eq. (6). First, the incomplete gamma bound comes as following:

$$p = \frac{1}{2}\left(1 - \Gamma\left(\frac{KM}{2}\cdot\frac{z^2}{2}\right)\right). \tag{7}$$

For small number of channel (i.e. K is smaller), incomplete gamma bound is quite tight.[8] However, for large number of channels, we may need more accurate approximation. This can be calculated using Sun's tube formula.[9] Now, let us define an inhomogeneous Gaussian random field

$$X_{HbO_2}(r) = \mathbf{u}_{HbO_2}(r)^H\mathbf{Z}. \tag{8}$$

where

$$\mathbf{u}_{HbO_2} = \frac{\mathbf{C}_{\hat{\boldsymbol{\beta}},HbO_2}^{1/2}\mathbf{B}(r)}{\sqrt{\mathbf{B}(r)^T\mathbf{C}_{\hat{\boldsymbol{\beta}},HbO_2}\mathbf{B}(r)}}. \tag{9}$$

where $\mathbf{B}$ denotes the vectors constructed from interpolating kernels, and $\mathbf{C}_{\hat{\boldsymbol{\beta}},HbO_2}$ is the error covariance matrix in estimating $\{\boldsymbol{\beta}_{HbO_2}^{(i)}\}_{i=1}^{K}$. Now we calculate the 2×2 *metric tensor matrix*:

$$\mathbf{R}(r) \triangleq E[\nabla X_{HbO_2}(r)\nabla^T X_{HbO_2}(r)]. \tag{10}$$

Then, finally we derive the following approximation:

$$P\left\{\max_{r\in\Psi} T_{HbO_2}(r) \geq z\right\} \simeq \kappa_0\psi_0(z), \tag{11}$$

where

$$\kappa_0 = |\mathcal{U}| = \int_\Psi \sqrt{|\det(\mathbf{R}(r))|}dr \tag{12}$$

and

$$\psi_0(z) = \frac{\Gamma\left(\frac{3}{2}\right)}{4\pi^{3/2}}\left(1-\Gamma\left(\frac{3}{2},\frac{z^2}{2}\right)\right). \tag{13}$$

The formula for p-value for the case of HbR can be derived in a same manner.

2.4 Temporal Preprocessing: Detrending and Estimating the Temporal Correlations

In many cases, there often exists global drifts of the NIRS measurements due to variety reasons, including subject movement during the experiment, blood pressure variation, long-term physiological changes or instrumental instability. Moreover, the amplitude of a global drift is often comparable to that of the signal from a brain activation. In order to eliminate the global trend to improve the signal-to-noise ratio, we employ the highpass filter based on a discrete cosine transform (DCT) which is currently implemented in SPM.[10]

After detrending, short-range temporal correlation still exists in NIRS data. In order to obtain the correct inference in Eq.(5), temporal correlation structure of NIRS has to be investigated. To solve this problem, we compared the "pre-coloring" with "pre-whitening" methods which was proposed for fMRI model.[10]

In case where temporal smoothing is strong enough to swamp any intrinsic temporal correlation, pre-coloring method is preferred. Specifically, if the full width at half maximum (FWHM) of smoothing kernel is sufficiently large, temporal correlation induced by the smoothing can be obtained without intrinsic temporal correlation:

$$\mathbf{\Lambda} = \mathbf{S\Sigma S}^T \approx \mathbf{SS}^T, \tag{14}$$

where $\mathbf{\Lambda}$ is a temporal correlation matrix, $\mathbf{\Sigma}$ denotes an intrinsic temporal correlation matrix, and $\mathbf{S}$ is a smoothing matrix which is typically derived from the canonical HRF or Gaussian smoothing kernel.[12] Because the transfer function of HRF is in the frequencies of modeled neuronal signals, we employ the canonical HRF for temporal smoothing of NIRS time-series.

An alternative way, pre-whitening, is to whiten the data using the smoothing matrix $\mathbf{S}$ which is derived from the intrinsic temporal correlation $\mathbf{\Sigma}$:

$$\mathbf{S} = \mathbf{K}^{-1}, \tag{15}$$

where $\mathbf{KK}^T = \mathbf{\Sigma}$ and $\mathbf{\Sigma}$ is estimated using ReML.[13] If estimated intrinsic temporal correlation is correct, the temporal correlation structure induced by smoothing can be an identity matrix as following:

$$\mathbf{\Lambda} = \mathbf{S\Sigma S}^T = \mathbf{I} \tag{16}$$

In the whitened model, since the error is identically and independent distributed, least square estimate $\hat{\boldsymbol{\beta}}$ corresponds to the maximum likelihood estimate.

2.5 Spatial Preprocessing: NIRS-fMRI Alignment

In order to localize the NIRS signal with respect to the cerebral cortex of anatomical MR image, the relationship between MR coordinates and real coordinates in 3-D digitizer has to be investigated. Horn's algorithm that gives a closed-form and least-square solution for this absolute orientation problem is employed.[11]

Let $p_{MR,i}$ and $p_{NIRS,i}$ denote a measured coordinate in the MR and 3-D digitizer system, respectively, where $i = 1, 2, \ldots n$ indexes the coordinates. Let s be a scale parameter, t be a translation vector, R be a rotation matrix. Then, our problem is to find the maximum likelihood estimate for these rigid transform parameters:

$$p_{MR} = s\mathbf{R}(p_{NIRS}) + t. \tag{17}$$

First, all measured coordinates are redefined with respect to centroids of their systems:

$$\begin{aligned} p'_{MR,i} &= p_{MR,i} - \bar{p}_{MR}, \\ p'_{NIRS,i} &= p_{NIRS,i} - \bar{p}_{NIRS}, \\ \bar{p}_{MR} &= \frac{1}{n}\sum_{i=1}^{n} p_{MR,i}, \\ \bar{p}_{NIRS} &= \frac{1}{n}\sum_{i=1}^{n} p_{NIRS,i}. \end{aligned} \tag{18}$$

Then, the translation vector and the scale factor are given by

$$\begin{aligned} \hat{t} &= \bar{p}_{MR} - s\mathbf{R}(\bar{p}_{NIRS}), \\ \hat{s} &= \frac{\sum_{i=1}^{n} p'_{MR,i} \cdot R(p'_{NIRS,i})}{\sum_{i=1}^{n} \|p'_{NIRS,i}\|^2}. \end{aligned} \tag{19}$$

Let $p'_i = (x'_i, y'_i, z'_i)^T$ and

$$\mathbf{A}_{MR,i} = \begin{bmatrix} 0 & -x'_i & -y'_i & -z'_i \\ x'_i & 0 & -z'_i & y'_i \\ y'_i & z'_i & 0 & -x'_i \\ z'_i & -y'_i & x'_i & 0 \end{bmatrix}, \quad \mathbf{B}_{NIRS,i} = \begin{bmatrix} 0 & -x'_i & -y'_i & -z'_i \\ x'_i & 0 & z'_i & -y'_i \\ y'_i & -z'_i & 0 & x'_i \\ z'_i & y'_i & -x'_i & 0 \end{bmatrix}. \tag{20}$$

If we define the matrix N as

$$\mathbf{N} = \sum_{i=1}^{n} \mathbf{B}^T_{NIRS,i}\mathbf{A}_{MR,i}, \tag{21}$$

the vector $\hat{q}$ which is directly related to the rotation parameters is the eigenvector corresponding to the maximum eigenvalue of the matrix $\mathbf{N}$. Let $\hat{q}$ be the quaternion $(q_0, q_x, q_y, q_z)^T$. Then, the rotation matrix is obtained as following:

$$\hat{\mathbf{R}} = \begin{bmatrix} (q_0^2 + q_x^2 - q_y^2 - q_z^2) & 2(q_x q_y - q_0 q_z) & 2(q_x q_z + q_0 q_y) \\ 2(q_y q_x + q_0 q_z) & (q_0^2 - q_x^2 + q_y^2 - q_z^2) & 2(q_y q_z - q_0 q_x) \\ 2(q_z q_x - q_0 q_y) & 2(q_z q_y + q_0 q_x) & (q_0^2 - q_x^2 - q_y^2 + q_z^2) \end{bmatrix} \tag{22}$$

After the relationship between the MR coordinates and real coordinates in 3-D digitizer is elicited based on the measured coordinates of marker capsules, the locations of optodes in the MR coordinate can calculated. The position of opotodes are projected onto the cortical cortex which is obtained from the segmented MR images.

3. NIRS-SPM: A NEW SPM TOOLBOX FOR NIRS

A new SPM appropriate to NIRS has been implemented as a "NIRS-SPM toolbox" based on SPM5 package (Wellcome Department of Cognitive Neurology, London, UK; http://www.fil.ion.ucl.ac.uk/spm). The toolbox runs under MATLAB (Mathworks, Natick, MA), providing various computational tools from temporal/spatial preprocessing to statistical analysis based on GLM and inference using global confidence region analysis (Fig. 1). Statistical results are superimposed onto the 3-D rendered SPM brain map and they can be compared with fMRI result, integrating with the conventional SPM for fMRI.

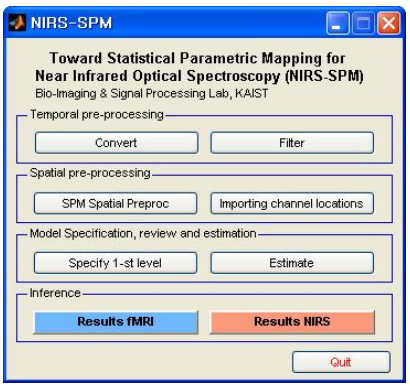

Figure 1. Main panel of the NIRS-SPM showing the four main groups of tools.

4. EXPERIMENTAL RESULTS

To evaluate the practical usefulness of proposed methods, we applied our new statistical analysis framework to right finger tapping experiment data. Experimental data were simultaneously acquired using a NIRS and fMRI system. Specifically, a NIRS system has 8 laser diodes and 4 detectors (Oxymon MK III, Artinis, Netherlands). In this system, two continuous wave light (781nm, 856nm) were emitted at each source fiber. The distance between source and detector was 3.5cm. MR images covering the whole brain were acquired with the echo planar imaging (EPI) sequence using a 3.0T MRI system (ISOL, Korea). In right finger tapping experiment, the subject were instructed to perform a finger flexion and extension repeatedly during task period. Because the primary motor cortex is the target region of right finger tapping task, optode-map was placed as shown in Fig.2(a). Figure 2(b) shows the optode positions in the MR coordinates after the spatial preprocessing step.

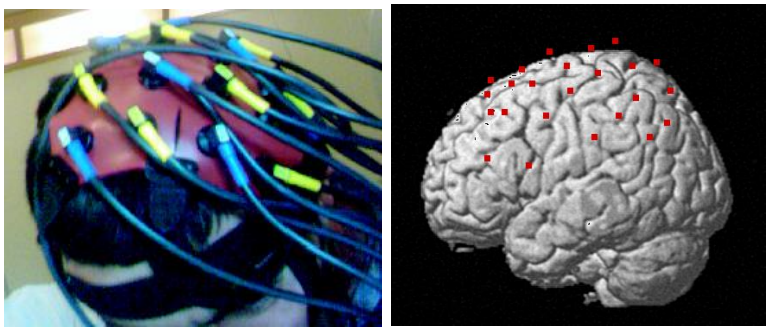

(a) (b)

Figure 2. (a) Experimental position of optode-map covering with primary motor cortex area for right finger tapping task and Broca's area for working memory task, (b) 24 NIRS channels located onto the SPM brain template.

Figures 3 show the GLM results from right finger tapping task. Activation maps of pre-colored and pre-whitened ΔHbO_2 are shown in Figs. 3(1st row) and (2nd row), respectively. Note that activation pattern of pre-colored ΔHbO_2 is more focused on the primary motor cortex than that of pre-whitened ΔHbO_2. The activation map using fOSA[5] with Gaussian random field model is shown in Figs. 3(a) and (d). fOSA cannot analyze the interpolated random field, so the estimated activated ares is very rough. Our t-maps of ΔHbO_2 over the threshold obtained using incomplete gamma bound and Sun's tube formula are shown in Figs. 3(b)(e) and (c)(f). respectively. Note that our activation pattern of ΔHbO_2 is fairly consistent with that of BOLD signal, as shown in Fig. 4. The incomplete gamma bound gives very optimistic estimate of the activated area, whereas the tube formula tells us that the more areas are activated by the finger tapping. Both of the results exhibits excellent correlation with the fMRI result. Furthermore, compared to fOSA results in Fig. 3(a) and (d), our method allows super-resolution localization.

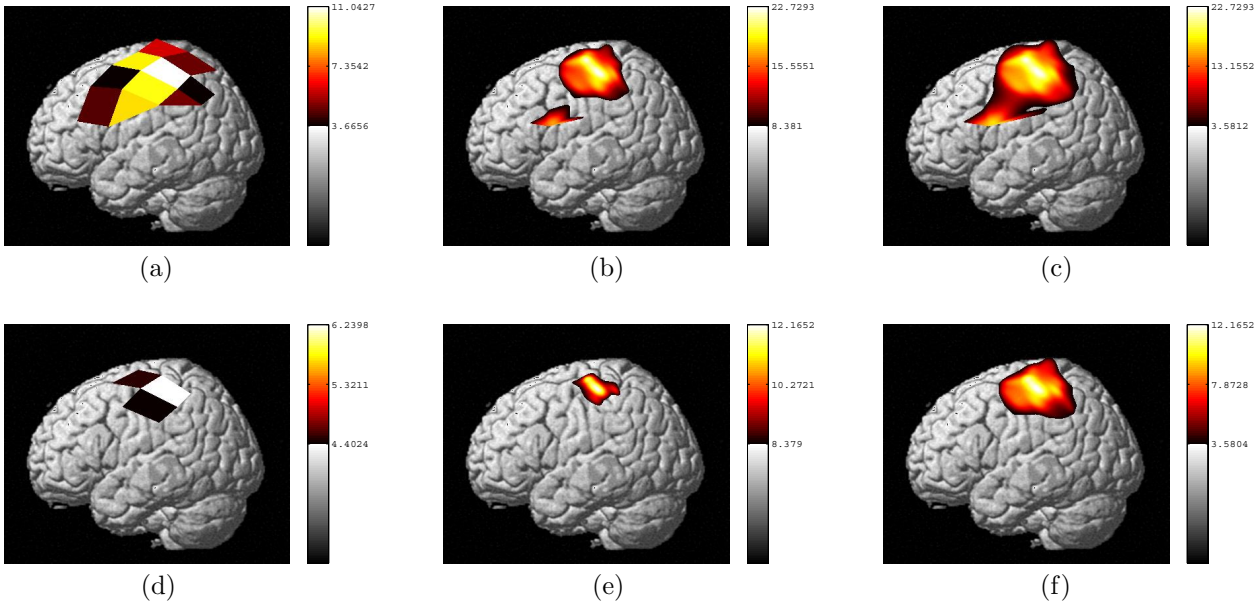

Figure 3. 1st row: Activation area of pre-whitened ΔHbO_2 using (a) fOSA,[5] (b) incomplete gamma bound, and (c) tube formula. 2nd row: Activation area of pre-colored ΔHbO_2 using (d) fOSA,[5] (e) incomplete gamma bound, and (f) tube formula. p-value is 0.01

Figure 4. SPM analysis of fMRI data (p-value: 0.01).

5. CONCLUSION

We developed a new public domain statistical toolbox called NIRS-SPM. In the main framework, NIRS-SPM successfully analyzed the NIRS data using GLM and calculated the p-value as the excursion probability which comes from the random field that are interpolated from the sparse measurement. In estimating the temporal correlation of NIRS, pre-coloring method was superior to pre-whitening method, due to the computational efficiency and sufficient temporal smoothing. In spatial preprocessing, NIRS-SPM localized the NIRS signal onto the cerebral cortex of anatomical MR image using Horn's algorithm. Experimental results from the right finger tapping task showed that the proposed methods can localize the activation of primary motor cortex very accurately.

ACKNOWLEDGMENTS

This research was supported in part by a Brain Neuroinformatics Research Program by Korean Ministry of Commerce, Industry and Energy.

REFERENCES

1. A. Villringer and U. Dirnafl, "Coupling of brain activity and cerebral blood flow: basis of functional neuroimaging," *Cerebrovasc. Brain Metab. Rev.* **7**, pp. 240–276, 1995.
2. F. Jobsis, "Noninvasive, infrared monitoring of cerebral and myocardial oxygen sufficiency and circulatory parameters," *Science* **198**, pp. 1264–1267, 1977.
3. M. L. Schroeter, M. M. Bucheler, K. Muller, K. Uludag, H. Obrig, G. Lohmann, M. Tittgemeyer, A. Villringer, and D. Y. von Cramon, "Towards a standard analysis for functional near-infared imaging," *NeuroImage* **21**, pp. 283–290, 2004.
4. M. M. Plichta, S. Heinzel, A. C. Ehlis, P. Pauli, and A. J. Fallgatter, "Model-based analysis of rapid event-related functional near-infrared spectroscopy (nirs) data: A parametric validation study," *NeuroImage* **35**, pp. 625–634, 2007.
5. P. H. Koh, D. E. Glaser, G. Flandin, S. Kiebel, B. Butterworth, A. Maki, D. T. Delpy, and C. E. Elwell, "Functional optical signal analysis: a software tool for near-infrared spectroscopy data processing incorporating statistical parametric mapping," *J. Biomed. Opt.* **12**, pp. 1–13, 2007.
6. K. J. Worsley and K. J. Friston, "Analysis of fmri time-series revisited-again," *NeuroImage* **2**, pp. 173–181, 1995.
7. K. J. Friston, A. P. Holmes, J.-B. Poline, C. J. Price, and C. D. Frith, "Dectecting activations in pet and fmri: Levels of inference and power," *NeuroImage* **40**, pp. 223–235, 1996.
8. J. C. Ye, P. Moulin, and Y. Bresler, "Asymptotic global confidence regions for 3-d parametric shape estimation in inverse problems," *IEEE Trans. Image Process.* **15**, pp. 2904–2919, 2006.
9. J. Sun, "Tail probabilities of the maxima of gaussian random fields," *Ann. Prob.* **21**, pp. 34–71, 1993.
10. K. J. Friston, J. Ashburner, S. Kiebel, T. Nichols, and W. Penny, *Statistical Parametric Mapping: The analysis of functional brain images*, Academic Press, Sandiego, CA, USA, 2006.
11. B. Horn, "Closed-form solution of absolute orientation using unit quaternions," *J. Opt. Soc. Amer. A* **4**, pp. 629–642, 1987.
12. K. J. Friston, O. Josephs, E. Zarahn, A. P. Holmes, S. Rouquette, and J.-B. Poline, "To smooth or not to smooth? bias and efficiency in fmri time-series analysis," *NeuroImage* **12**, pp. 196–208, 2000.
13. K. J. Friston, W. D. Penny, C. Phillips, S. Kiebel, G. Hinton, and J. Ashburner, "Classical and bayesian inference in neuroimaging: theory," **16**, pp. 465–483, 2002.